



## Oblique helicoidal state of the twist-bend nematic doped by chiral azo-compound

Vitalii Chornous, Alina Grozav, Mykhailo Vovk, Daria Bratova, Natalia Kasian, Longin Lisetski & Igor Gvozдовskyy

To cite this article: Vitalii Chornous, Alina Grozav, Mykhailo Vovk, Daria Bratova, Natalia Kasian, Longin Lisetski & Igor Gvozдовskyy (2023): Oblique helicoidal state of the twist-bend nematic doped by chiral azo-compound, *Liquid Crystals*, DOI: [10.1080/02678292.2023.2200267](https://doi.org/10.1080/02678292.2023.2200267)

To link to this article: <https://doi.org/10.1080/02678292.2023.2200267>

 View supplementary material 

 Published online: 24 Apr 2023.

 Submit your article to this journal 

 Article views: 59

 View related articles 

 View Crossmark data 



# Oblique helicoidal state of the twist-bend nematic doped by chiral azo-compound

Vitalii Chornous <sup>a</sup>, Alina Grozav <sup>a</sup>, Mykhailo Vovk <sup>b</sup>, Daria Bratova <sup>c,d</sup>, Natalia Kasian <sup>e,f</sup>, Longin Lisetski <sup>e</sup> and Igor Gvozдовskyy <sup>d</sup>

<sup>a</sup>Department of Medical and Pharmaceutical Chemistry, Bukovinian State Medical University, Chernivtsi, Ukraine; <sup>b</sup>Department of Mechanisms of Organic Reactions, Institute of Organic Chemistry of the National Academy of Sciences of Ukraine, Kyiv, Ukraine; <sup>c</sup>Department of Information and Measuring Technologies, National Technical University of Ukraine "Igor Sikorsky Kyiv Polytechnic Institute", Kyiv, Ukraine; <sup>d</sup>Department of Optical Quantum Electronics, Institute of Physics of the National Academy of Sciences of Ukraine, Kyiv, Ukraine; <sup>e</sup>Department of Nanostructured Materials, Institute for Scintillation Materials of STC "Institute for Single Crystals" of the National Academy of Sciences of Ukraine, Kharkiv, Ukraine; <sup>f</sup>Faculty of Physics, Warsaw University of Technology, Warsaw, Poland

## ABSTRACT

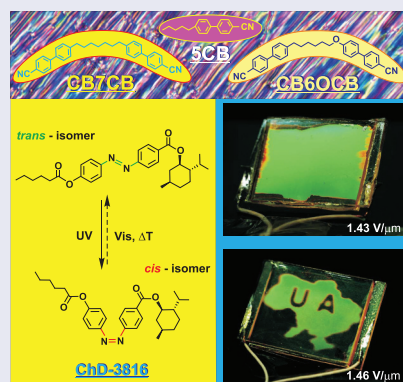
A novel light-sensitive chiral dopant ChD-3816 (an azo-compound containing 4-hexanoyloxyphenyl and 2-isopropyl-5-methylcyclohexylbenzoate moieties) was used for inducing helical twisting in  $N_{tb}$ -forming mixtures of CB7CB/CB6OCB with 5CB added to decrease the phase transition temperatures. The effects of ChD-3816 upon phase transition temperatures, as well as effects of its concentration on the measured values of helical twisting, were determined. Most of the measured parameters could be varied due to light-induced *trans-cis* isomerisation of ChD-3816. Under electric field, selective reflection spectra in the visible range were obtained for the emerging oblique helicoidal cholesteric structures ( $Ch_{OH}$ ), with the wavelengths controllable both by electric field and appropriate UV irradiation. Possible applications for dynamic formation of contrast images are discussed.

## ARTICLE HISTORY

Received 14 March 2023  
Accepted 4 April 2023

## KEYWORDS

Phase transition; twist-bend nematic phase; chiral twist-bend phase; cholesteric; chiral azo-compound



## 1. Introduction

Though liquid crystals as a new state of matter were discovered in the course of studies of cholesterol esters about 160 years ago [1–4], the search for new cholesteric liquid crystals (CLCs) still remains relevant due to their wide practical applications. Nowadays, CLCs are no more directly related to cholesterol esters or other steroid compounds, but are typically mixtures consisting of a host nematic liquid crystal (LC) which, upon dissolution of a chiral dopant (ChD) therein, is self-reassembled forming a helicoidal structure (Figure 1(a)). In this

structure, generally known as a chiral nematic ( $N^*$ ) phase, the molecules align perpendicularly to the cholesteric helical axis [5]. The helicoidal structure is characterised by the pitch  $P_0$ , which depends on the helical twisting power (HTP,  $\beta$ ) of ChDs and their concentration  $C$  in nematic LCs. It can be expressed as  $\beta = (P_0 \times C)^{-1}$  [6,7]. Thus, for the cholesteric phase induced by a ChD with concentration  $C$ , the wave number is written as  $q_0 = \pm 4\pi \times \beta \times C$ , where  $\beta$  is the efficiency of the dopant to induce a cholesteric phase with the helical pitch  $P_0 = 2\pi/|q_0|$ . The helicoidal structure can be right-

**CONTACT** Igor Gvozдовskyy  igvozdz@gmail.com

 Supplemental data for this article can be accessed online at <https://doi.org/10.1080/02678292.2023.2200267>.

© 2023 Informa UK Limited, trading as Taylor & Francis Group

handed ( $q_0 > 0$ ) or left-handed ( $q_0 < 0$ ) depending on both the nature of ChD molecules and their interaction with nematic LC molecules [5].

The search for novel cholesteric and other helically twisted liquid crystal systems led to many interesting developments with promising practical applications. Thus, in recent years great attention was paid to nematic hosts with very low values of the bend elastic constant  $K_{33}$ . This interest was partially based on theoretical predictions of specific cholesteric-like states based on LCs with the bend elastic constant  $K_{33}$  being much lower than the twist elastic constant  $K_{22}$  [8,9]. Later, it was assumed [10] that banana-shaped mesogenic molecules, inducing a local bend of the nematic director, could give rise to a phase with negative bend elastic constant, predicting a lower symmetry nematic phase characterised by symmetry breaking transition from uniform texture to spontaneous periodic distortion, either oscillating splay-bend or conical twist-bend helix. Another tentative model and mechanism describing possible cholesteric helix distortions of the ‘oblique helicoidal’ nature caused by ChDs of a specific nature (*e.g.* small anisotropy and significant molecular biaxiality) were proposed, considering the relationship between elastic deformation fields and the director of quasi-nematic layer [11].

In this work, we used recently described twist-bend nematic ( $N_{tb}$ ) LCs [12–14], with a low value of bend constant  $K_{33}$  to obtain chiral twist-bend nematics ( $N_{tb}^*$ ) by adding a small quantity of ChD [15,16].

As it could be expected, we have experimentally found that our LC mixtures possessing the  $N_{tb}^*$  phase can form, at temperatures above the  $N_{tb}^* - N^*$  phase transition, a specific cholesteric state under AC electric field known as the helicoidal structure of cholesteric (or  $Ch_{OH}$  for short) [15,16]. In this state, the molecules are twisted around the cholesteric helical axis with a certain oblique angle of  $\theta$  (Figure 1(b)), as distinct from the conventional CLCs, where  $\theta = 90^\circ$  [5,9]. Under applied electric field larger than the threshold field ( $E_{NC}$ ) the oblique helicoidal structure (Figure 1(b)) undergoes the transformation to the homeotropically aligned nematic. This threshold field can be described as follows [8,15]:

$$E_{NC} = \frac{2\pi \cdot K_{22}}{P_0 \cdot \sqrt{\varepsilon_0 \cdot \Delta\varepsilon \cdot K_{33}}}, \quad (1)$$

where  $\varepsilon_0$  is the constant of vacuum permittivity and  $\Delta\varepsilon$  is the dielectric anisotropy of the LC mixture,  $K_{22}$  and  $K_{33}$  are twist and bend elastic constants, respectively;  $P_0$  is the length of cholesteric pitch of  $N^*$  phase of the  $N_{tb}^*$ -forming mixture in the absence of applied electric field.

The  $Ch_{OH}$  state can show selective reflection of light (so-called Bragg diffraction) in the visible spectral range under certain conditions, namely temperature  $T_B$  and an electric field  $E_B$ . The maximum of wavelength  $\lambda_{max}$  of the reflected light can be tuned by changing of temperature, applied voltage and frequency of the electric field

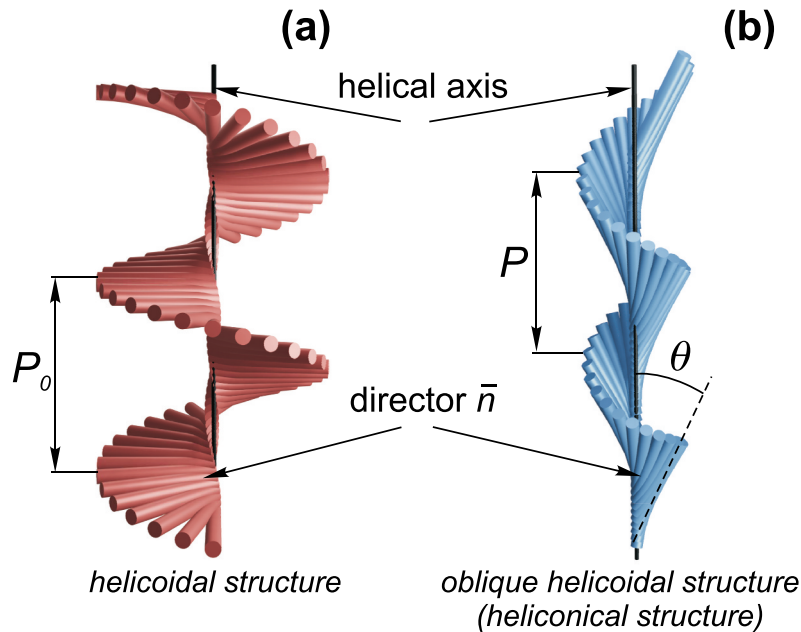


**Figure 1.** (Colour online) Schematic illustration of the structure in which local orientation of LC molecules (director  $\vec{n}$ ) rotates around the helical axis: (a) perpendicularly in the absence of electric fields for helicoidal cholesterics ( $N^*$ ) with the helix pitch length  $P_0$ , and (b) with an oblique angle  $\theta$  for heliconical cholesterics ( $Ch_{OH}$ ) under electric field  $E$ . The length of the heliconical helix pitch  $P$  and oblique angle  $\theta$  increase with decreasing applied electric field  $E$ .

[15–21]. Besides, when the electric field  $E_B$  is decreased, there is also a threshold field ( $E_{N^*C}$ ), when the oblique helicoidal structure (Figure 1(b)) transforms to conventional helicoidal structure (*i.e.*  $\theta = 90^\circ$ ), which is reflected by the appearance of the focal conic texture leading to intense light scattering. This threshold electric field can be expressed as [8]:

$$E_{N^*C} \approx E_{NC} \cdot \frac{K_{33}}{K_{22} + K_{33}} \left[ 2 + \sqrt{2 \cdot \left( 1 - \frac{K_{33}}{K_{22}} \right)} \right] \quad (2)$$

Thus, the main condition for the existence of  $\text{Ch}_{\text{OH}}$  structure is a non-zero applied electric field  $E$  at a certain temperature  $T$  (*i.e.* when  $K_{33}/K_{22} < 1/2$  [9]), when the following inequality is satisfied:

$$E_{N^*C} \leq E \leq E_{NC} \quad (3)$$

However, it should be noted that in reality the  $\text{Ch}_{\text{OH}}$  structure can display the selective Bragg reflection of light in UV, visible (*e.g.* from  $\lambda_1$  to  $\lambda_2$ ) and IR ranges, and this general case is expressed in the Inequality (3). Therefore, the Bragg reflection in the visible range will be observed in a somewhat narrower interval of electrical field  $E$  than suggested by the Inequality (3) and can be written as follows:

$$E_B^{\lambda_2} \leq E \leq E_B^{\lambda_1}, \quad (4)$$

where  $E_B^{\lambda_1}$  and  $E_B^{\lambda_2}$  are values of electric fields  $E$  under which the Bragg reflection of light is observed in the visible range ( $\lambda_1 < \lambda_2$ ).

The detailed studies of the oblique helicoidal cholesterics and their applications are described in Refs [15–24].

The idea to use photosensitive chiral dopants to obtain  $N^*_{\text{tb}}$ -forming mixtures that, above the  $N^*_{\text{tb}} - N^*$  transition display the oblique helicoidal cholesteric state under applied field was recently realised [22–24]. The oblique helicoidal cholesterics consisting of both non-chiral azoxybenzene derivative [22,23] and a chiral photosensitive compound [24] were characterised by an additional useful property, namely, photo-controllable tuning of selective reflected wavelength.

The  $N_{\text{tb}}$ -forming systems are usually characterised by a sequence of twist-bend nematic – nematic – isotropic ( $N_{\text{tb}} - N - \text{Iso}$ ) phase transitions [17,18,20]. As it was theoretically predicted in [25] the adding of chiral and achiral dopants to such systems should affect the phase diagrams and helical twisting. Experimentally it was shown that the decreasing of the temperatures of phase transitions is also obtained when adding both the nematic 5CB and different ChDs [26].

In this manuscript we describe chiral  $N_{\text{tb}}$ -based phases doped with light-sensitive chiral dopant in

various concentrations that display the oblique helicoidal cholesteric state under applied electric field. The influence of the concentration of light-sensitive chiral dopant and irradiation time on temperatures of phase transitions of  $N^*_{\text{tb}}$  and the magnitude of the electric field needed to tune the wavelength of the Bragg reflection in oblique helicoidal cholesteric state will be described.

## 2. Experiment

To obtain a  $N_{\text{tb}}$ -forming system with low temperature phase transitions, we used the three-component nematic mixture containing two achiral liquid crystals dimers, namely 1',7'-bis-4-(4-cyanobiphenyl-4'-yl)heptane (CB7CB) and 1-(4-cyanobiphenyl-4'-yloxy)-6-(4-cyanobiphenyl-4'-yl)hexane (CB6OCB) and monomer nematic 4-pentyl-4'-cyanobiphenyl (K15 or 5CB) in the weight ratio of (39:19:42). Both twist-bend nematics were obtained from Synthon Chemicals GmbH & Co (Wolfen, Germany), while the nematic 5CB was synthesised and purified before using at the STC 'Institute of Single Crystals' (Kharkiv, Ukraine). It is known that CB7CB possesses a uniaxial nematic N phase in a temperature range of 103–116 °C [12,27,28], while CB6OCB possesses a uniaxial N phase in a temperature range of 109–157 °C [27–31]. The temperature dependence of the elastic, dielectric constants and refractive indices twist-bend nematic CB7CB was measured in Ref. [32]. Chemical structures of the nematic molecules forming the basic  $N_{\text{tb}}$  mixture are shown in Figure 2(a).

To induce chirality in the twist-bend nematic, we used (1R,2S,5R)-2-isopropyl-5-methylcyclohexyl-4- $\{(E)-[4-(\text{hexanoyloxy})\text{phenyl}]\text{diazanyl}\}$ benzoate (or ChD-3816 for short) synthesised in Bukovinian State Medical University (Chernivtsi, Ukraine) as a left-handed light-sensitive chiral dopant (Supplementary Material). Chemical structures of the *trans*- and *cis*-isomers of the ChD-3816 molecule are shown in Figure 2(b).

To study the influence of the chiral dopant on the properties of the emerging LC phases, the three-component nematic mixture was doped by ChD-3816 within concentration range 6–13 wt. %.

To obtain planar alignment, *n*-methyl-2-pyrrolidone solution of the polyimide PI2555 (HD MicroSystems, USA) [33] in proportion 10:1 was used. PI2555 films were spin-coated (6800 rpm, 10 s) on glass substrates (microscope slides, made in Germany) covered by indium tin oxide (ITO) layer. Substrates were dried at 80 °C for 15 min, followed

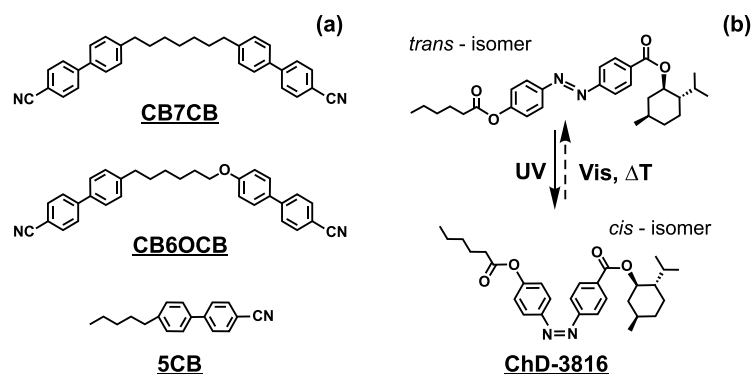


**Figure 2.** Schematic image of molecular structures of the nematics: CB7CB, CB6OCB and 5CB (a) and the light-sensitive chiral dopant ChD-3816 in *trans*- and *cis*-forms (b).

by annealing at 180 °C for 30 min. The thin polyimide layers were unidirectionally rubbed  $N_{rub} = 15$  times to provide their strong azimuthal anchoring energy [34].

To measure the length of cholesteric pitch  $P_0$  of the  $N^*$  phase, the Grandjean-Cano method [5] was used. The wedge-like LC cells were assembled by using pair glass substrates covered with PI2555 film having opposite rubbing directions and dimensions  $10 \times 15 \text{ mm}^2$ . The thickness of cells  $d$  was set to 3–10  $\mu\text{m}$  by Mylar spacer.

The plane-parallel LC cells were assembled with a thickness set by 20  $\mu\text{m}$  diameter Mylar spacer and controlled by the interference method, measuring the transmission spectrum of the empty cell by means of the spectrometer Ocean Optics USB4000 (Ocean Insight, USA, California). LC cells were filled by capillary action in the isotropic phase (Iso) of  $N^*_{tb}$  and further slowly cooled.

To study the influence of electric field on LC cells filled by  $N^*_{tb}$  mixtures, the alternating voltage within the range 0–100 V and frequency 1 kHz was used. The experiments were carried out at constant temperature within the 27–44 °C range.

For irradiation of LC mixtures containing the light-sensitive ChD-3816, the UV lamp with  $\lambda_{\text{max}} = 365 \text{ nm}$ , ensuring the intensity (energy illuminance) in the plane of the sample  $I \sim 14 \text{ mW/cm}^2$  was used. The illumination of LC cells was carried out from a distance of 30 mm through masks of arbitrary shape.

The temperatures of phase transitions of the mixtures containing various concentration of ChD-3816 were studied in a thermostable heater based on a temperature regulator MikRa 603 (LLD ‘MikRa’, Kyiv, Ukraine) equipped with a platinum resistance thermometer Pt1000 (PJSC ‘TERA’, Chernihiv, Ukraine). The temperature measurement accuracy was  $\pm 0.1 \text{ }^\circ\text{C/min}$ .

The phase textures were observed by means of the polarising optical microscope (POM) BioLar PI (Warsaw, Poland) equipped by digital camera Nikon D80.

### 3. Results and discussions

#### 3.1. Phase transitions of nematic/chiral nematic mixtures with the low-temperature twist-bend phase

In this section, we discuss the effects of the light-sensitive chiral dopant ChD-3816 containing azo-fragment on the temperatures of  $N_{tb} - N - \text{Iso}$  phase transitions of the CB7CB:CB6OCB:5CB mixture.

In case of the  $N_{tb}$  phase formed by flexible achiral dimers like CB7CB, the temperature of phase transition can be lowered by adding a certain concentration of nematic 5CB consisting of rod-like molecules [35]. Recently it was shown that for  $N_{tb}$  mixture consisting of two flexible achiral dimers CB7CB and CB6OCB in ratio (1:1) the temperatures of phase transitions were decreased upon adding both the nematic 5CB and different ChDs (e.g. R-811 and cholesteryl oleyl carbonate) [26].

As shown in Ref. [16], three-component nematic mixtures CB7CB:CB6OCB:5CB in certain ratios, when doped with a small concentration of left-handed ChD S-811, possess the  $N^*$  phase in a broad temperature range including near-room temperatures, and under applied electric field the heliconical cholesteric phase  $\text{Ch}_{OH}$  is observed. Based on these studies, we prepared an  $N_{tb}$ -forming mixture CB7CB:CB6OCB:5CB in weight ratio (39:19:42) doped with various concentrations of light-sensitive ChD-3816, with the aim of obtaining the  $\text{Ch}_{OH}$  state under application of an electric field in a broad temperature range.

Figure 3 shows the diagram of phase transitions of the basic  $N_{tb}$  mixture CB7CB:CB6OCB:5CB in weight ratio (39:19:42) during heating and cooling processes.

The sequential textures of the basic  $N_{tb}$  mixture during heating process in POM are shown in Figure 4. The  $N_{tb}$  phase exists up to about 38 °C and the typical stripes texture is observed (Figure 4(a,b)). The  $N_{tb}$  phase, placed between crossed polariser (P) and analyser (A), is characterised by birefringence as a typical nematic LCs. Figure 4(a) shows the  $N_{tb}$  phase when the rubbing direction coincides with the plane of the polarisation of P and no transmission of light is observed. The rotation of the sample by 45° leads to an increase in the sample transmittance owing to birefringence (Figure 4(b)). The planar texture of the N phase (Figure 4(d)) is observed in the wide temperature range about 40 °C (Figure 3)

It was experimentally found that adding certain concentration of the left-handed chiral dopant ChD-3816 within range 6–13 wt. % to the basic  $N_{tb}$  gives rise to the

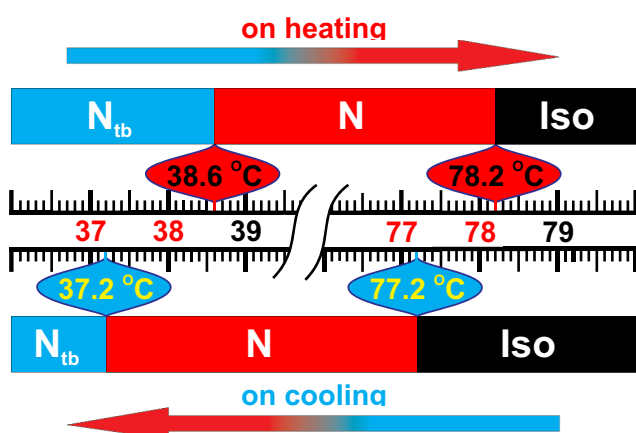


Figure 3. (Colour online) Schematic diagram of the sequence transitions on heating and cooling of: (a) basic  $N_{tb}$  phase, containing of CB7CB, CB6OCB and 5CB in weight ratio (39:19:42). The rate of the temperature change during the heating/cooling process was 0.1 °C/min.

formation  $N_{tb}^*$ , possessing the  $Ch_{OH}$  state under application of an electric field.

It could be expected that, in the same way as in [26], the lowering of the phase transition temperatures of the basic  $N_{tb}$  mixture would be realised by increasing the concentration of ChD-3816. The obtained results are presented in Table 1.

Figure 5 shows the sequence of textures during heating process of the chiral twist-bend phase  $N_{tb}^*$  based on basic  $N_{tb}$  doped with 8 wt. % ChD-3816. The blocky texture of  $N_{tb}^*$  phase is shown in Figure 5(a). Due to the presence of chiral molecules, the  $N_{tb}^* - N^*$  phase transition occurs at lower temperatures than with undoped  $N_{tb}$  phase (Table 1). Before the  $N_{tb}^* - N^*$  transition the polygonal texture appears (Figure 5(b)). For the  $N^*$  phase, the Grandjean-Cano (planar) texture (with oily streaks typical for cholesteric textures) is observed (Figure 5(c)).

Dependence of the phase transition temperatures on the ChD-3816 concentration is shown in Figure 6(a).

We see that the phase transition temperatures are decreasing upon addition of ChD-3816. A small hysteresis on heating and cooling of  $N_{tb}^*$  is observed. The  $N^*$  phase exists in the wide temperature range about 25–32 °C, depending on concentration of ChD-3816 both on heating and cooling. The widest possible range of temperatures of existence of the  $N^*$  phase ( $\Delta T_{N^*}$ ) is observed for concentration range 8–10 wt. % of ChD-3816 (Figure 6(b)), which could be important for various applications.

### 3.2. Oblique helicoidal cholesterics containing the light-sensitive ChD-3816

With all tested concentrations  $C$  of ChD-3816 in the basic  $N_{tb}$  mixture, no selective Bragg reflection of light could be observed in the  $N^*$  phase without the applied electric field; and the helical pitch  $P_0$  is a bit too high to detect

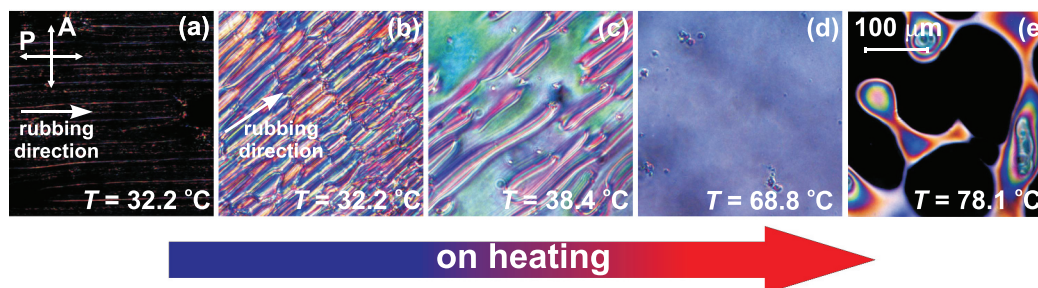
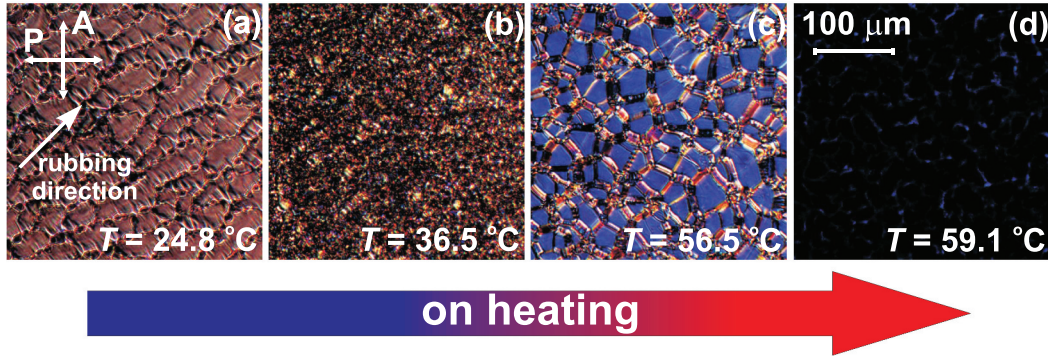
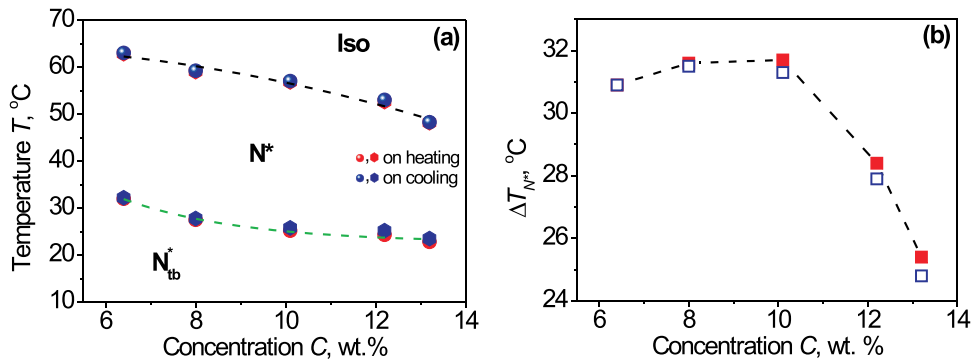


Figure 4. (Colour online) Photographs of the textures of the basic  $N_{tb}$  mixture containing 39 wt. % CB7CB, 19 wt. % CB6OCB and 42 wt. % 5CB in 21.4  $\mu\text{m}$  LC cell on heating: (a)  $N_{tb}$  phase at 32.2 °C when plane polarization of polarizer P coincides with rubbing direction; (b)  $N_{tb}$  phase at 32.2 °C with the 45° angle between the polarization plane of polarizer P and rubbing direction; (c)  $N_{tb} - N$  phase transition at 38.4 °C; (d) N phase at 68.8 °C, and (e) N - Iso phase transition at 78.1 °C. LC cell was placed between crossed polarizer (P) and analyzer (A) of POM. The rubbing direction of PI2555 layers (indicated by arrow) is rotated by about 45° with respect to the polarizers.

**Table 1.** Temperatures of phase transitions of the  $N_{tb}$ -forming mixture CB7CB:CB6OCB:5CB in weight ratio (39:19:42) containing different concentrations of ChD-3816 on heating and cooling.

Concentration of ChD-3816, wt. %	$T_{N_{tb}/N_{*tb}-N/N_{*r}}$ °C		$T_{N/N_{*}-Iso}$ °C	
	on heating	on cooling	on heating	on cooling
0	38.6	37.2	78.2	77.2
6.4	32	32.2	62.9	63.1
8	27.5	27.8	59.1	59.3
10.1	25.2	25.8	56.9	57.1
12.2	24.3	25.2	52.7	53.1
13.2	22.8	23.5	48.2	48.3

**Figure 5.** (Colour online) Photographs of the textures of the  $N_{*tb}$  phase containing the basic  $N_{tb}$  mixture doped with 8 wt. % ChD-3816 during heating process: (a) blocky texture of the  $N_{*tb}$  phase at 24.8 °C; (b) polygonal texture of the  $N_{*tb}$  phase at 36.5 °C; (c) Grandjean-Cano texture and oily streaks of the  $N_{*}$  phase; (d)  $N_{*}$  – Iso phase transition at 59.1 °C. LC cell was placed between crossed polarizer (P) and analyzer (A) of POM. The rubbing direction (indicated by arrow) of PI2555 layers is rotated by about 45° with respect to the polarizers. Thickness of the LC cell was 20.8  $\mu$ m. LC cell was placed between crossed polarizer (P) and analyzer (A) of POM. The rubbing direction (indicated by arrow) of PI2555 layers is rotated by about 45° with respect to the polarizers.**Figure 6.** (Colour online) Dependence of the temperatures of phase transitions  $N_{*tb}$  –  $N_{*}$  and  $N_{*}$  – Iso (a) and the temperature range of the  $N_{*}$  phase (b) on concentration of the ChD-3816 on heating (red symbols) and cooling (blue symbols).

wavelength  $\lambda_{max}$  in the visible range. Figure 7(a) shows the measured cholesteric helix pitch  $P_0$  as function of concentration of ChD-3816 at 34 °C (*i.e.* at this temperature, the  $N_{*}$  phase is observed for all studied concentrations of ChD-3816 given in Table 1).

No noticeable changes in  $P_0$  with temperature were noted in the entire range of the existence of  $N_{*}$  phase. The decrease of the length of cholesteric pitch  $P_0$  in the  $N_{*}$  phase with increasing concentration of the ChD-3816 happens without selective Bragg reflection of light in visible spectrum similarly to the

conventional induced cholesterics formed by small concentration of chiral dopant (*e.g.* see Figure 3S1(a) in Supplementary Material for the cholesteric mixture containing nematic E7 and the same ChD-3816 as in our study).

Figure 7(b) shows the linear dependence of the reciprocal cholesteric pitch  $1/P_0$  on concentration of ChD-3816. As the linear dependence  $1/P_0(C)$  passes through the origin of coordinates, the value  $HTP \sim 0.082$  ( $\mu\text{m} \times \text{wt. \%})^{-1}$  of ChD-3816 in basic  $N_{tb}$  host was calculated. Thus, the HTP value of ChD-3816 in the basic  $N_{tb}$  host

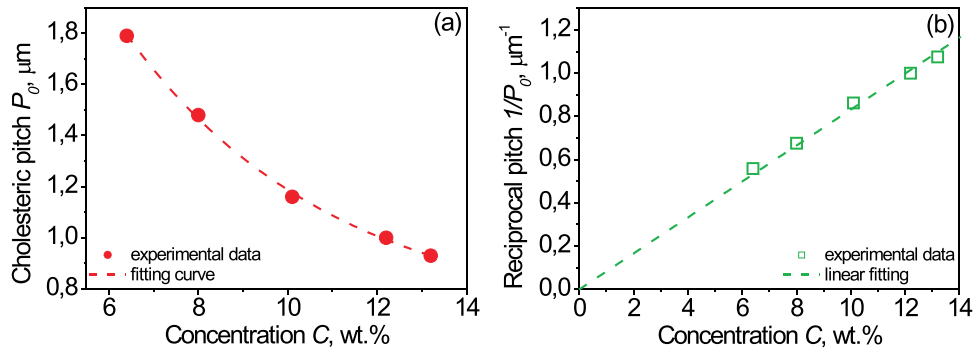


**Figure 7.** (Colour online) Dependence of cholesteric pitch  $P_0$  (a) and reciprocal cholesteric pitch  $1/P_0$  (b) on concentration  $C$  of the ChD-3816 in the  $N_{tb}$ -forming mixture CB7CB:CB6OCB:5CB in weight ratio (39:19:42) in  $N^*$  phase at 34 °C in the absence of the applied electric field.

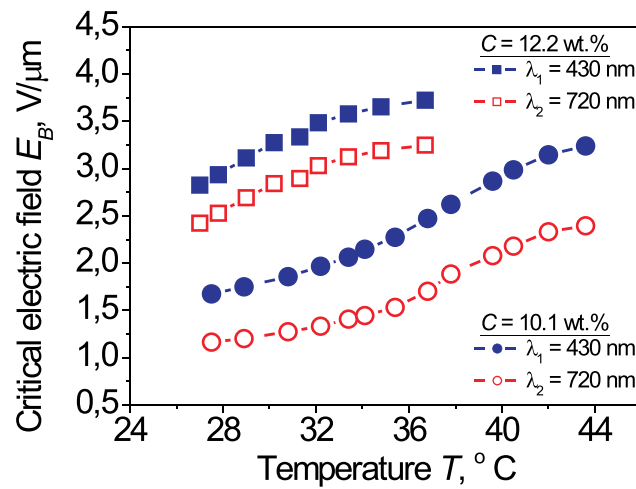


**Figure 8.** (Colour online) Dependence of the critical electric field  $E_B$  on the temperature  $T$  of the  $Ch_{OH}$  based on  $N_{tb}$  mixture (CB7CB:CB6OCB:5CB) with weight ratio (39:19:42) and ChD-3816 with concentrations: 10.1 wt. % (circles symbols) and 12.2 wt. % (squares symbols). Critical electric field value  $E_B$  is at:  $\lambda_1 = 430$  nm (solid blue symbols) and  $\lambda_2 = 720$  nm (opened red symbols). The thickness of the LC cell was 20.5  $\mu\text{m}$  (circles symbols) and 20.1  $\mu\text{m}$  (squares symbols), respectively.

is slightly smaller than in the nematic host E7 (Supplementary Material, Figure 3S2).

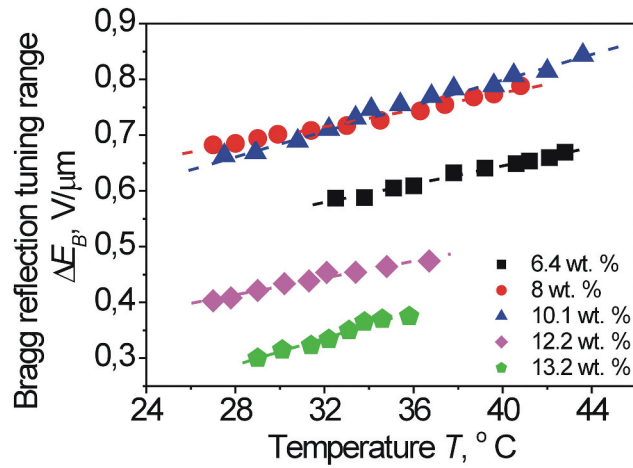
It is quite obvious that within the temperature range  $\Delta T_{N^*}$  (Figure 6(b)) the oblique helicoidal cholesteric state displaying selective Bragg reflection of light in the visible spectral range appears at the critical applied field  $E_B$ , which is below the threshold electric field  $E_{NC}$  and above  $E_{N^*C}$ . To obtain the temperature range  $\Delta T_{ChOH}$  of the  $Ch_{OH}$  state, the measurements of the critical applied voltage  $U_B$  (or electric field  $E_B = U_B/d$ ) under tuning at two wavelengths (*i.e.*  $\lambda_1 = 430$  and  $\lambda_2 = 720$  nm) for various temperatures  $T$ , were carried out.

Figure 8 shows the dependence of the critical electric field  $E_B$  on temperature  $T$  of the  $Ch_{OH}$  at different concentrations of ChD-3816 in the basic  $N_{tb}$  mixture. The increasing of the  $Ch_{OH}$  temperature leads to the switching-on of the Bragg reflection at higher  $E_B$ . The values of the critical electric field  $E_B^{\lambda_1=430}$  and  $E_B^{\lambda_2=720}$

required to tune on the Bragg reflection increase with increasing temperature of the  $Ch_{OH}$  phase. With higher chiral dopant concentration  $C$ , the value of critical electric field  $E_B$  increases.

It should be noted that the range of the applied field  $\Delta E_B$  (*i.e.*  $\Delta E_B = E_B^{\lambda_1=430} - E_B^{\lambda_2=720}$ ) required to tune on the selective reflection in the range of the visible light spectrum also depends on both the concentration of ChD-3816 and the temperature  $T$  of  $Ch_{OH}$ .

Figure 9 shows the dependence of the range of critical electric field  $\Delta E_B$  on temperature  $T$  of the  $Ch_{OH}$  with various concentrations of ChD-3816. The increasing  $Ch_{OH}$  temperature  $T$  leads to a slight increase in the range of  $\Delta E_B$ , which is in a good agreement with results reported in [18]. The main cause of this is the increase in the bend elastic constants  $K_{33}$  of twist-bend nematic CB7CB, as, *e.g.* measured experimentally in [32]. Thus, we may assume that both for basic  $N_{tb}$  and for  $N_{tb}^*$



**Figure 9.** (Colour online) Dependence of the range of critical electric field  $\Delta E_B$  on temperature of the  $\text{Ch}_{\text{OH}}$  for ChD-3816 concentration: 6.4 wt. % (solid black squares); 8 wt. % (solid red circles); 10.1 wt. % (solid blue triangles); 12.2 wt. % (solid magenta diamonds); 12.2 wt. % (solid green pentagons).

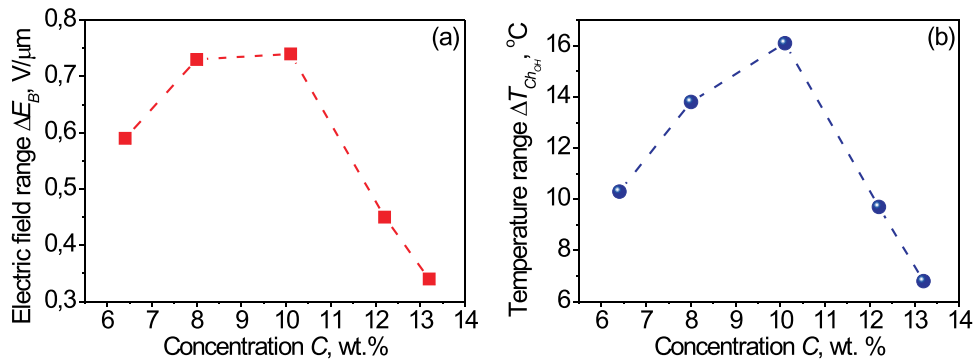


**Figure 10.** (Colour online) Dependence of the critical electric field range  $\Delta E_B$  at 34 °C (a) and temperature range of the  $\text{Ch}_{\text{OH}}$  state  $\Delta T_{\text{Ch}_{\text{OH}}}$  (b) on concentration of ChD-3816 in the studied oblique helicoidal cholesteric.

mixtures doped with various concentrations of ChD-3816, the bend elastic constant  $K_{33}$  increases with temperature.

Figure 10 shows both the range of critical electric field  $\Delta E_B$  for 34 °C (a) and temperature interval  $\Delta T_{\text{Ch}_{\text{OH}}}$  (b) of the  $\text{Ch}_{\text{OH}}$  state where Bragg reflection of light is observed within the visible range for various concentrations of the ChD-3816. The widest range of critical electric field  $\Delta E_B$  is observed for concentrations within the range about 8–10 wt. % (Figure 10(a)). The widest temperature range is about 16 °C for the  $\text{Ch}_{\text{OH}}$  containing 10 wt. % ChD-3816 (Figure 10(b)). We can conclude that the  $\text{N}^*_{\text{tb}}$ -forming mixture with 8–10 wt. % of the ChD3816 may become the most preferred choice option for many possible applications.

The photographs of the 20.5  $\mu\text{m}$  LC cell filled by the  $\text{N}^*_{\text{tb}}$ -forming mixture with 10.1 wt. % of ChD-3816 in the  $\text{Ch}_{\text{OH}}$  state (with selective Bragg reflection in the visible spectrum) are shown in Figure 11(a–c) for various values of electric field  $E$  ( $f = 1$  kHz).

Figure 12(a) shows the dynamics of the transmission spectrum of the  $\text{Ch}_{\text{OH}}$  state recorded by spectrometer Ocean Optics USB4000. The sequential shifting of the selective reflection wavelength towards the range with longer wavelengths (*i.e.* so-called red shift) under decreasing electric field is shown in Figure 12(b).

### 3.3. Phase transitions of UV-irradiated $\text{N}^*_{\text{tb}}$

In this section, we will consider the effects of UV irradiation on the phase transition temperatures of the  $\text{N}^*_{\text{tb}}$ -forming mixtures. As chiral molecules of ChD-3816 are photosensitive, the transformation of the rod-like *trans*-isomer to a bended *cis*-isomer with a dramatic change in molecular geometry was expected to cause the change in the HTPs of these isomers. This, in turn, enables us, on the one hand, to tune the length of cholesteric pitch  $P_0$  by the light exposure and, on the other hand, to change the order parameters by varying the temperatures of the phase transitions.

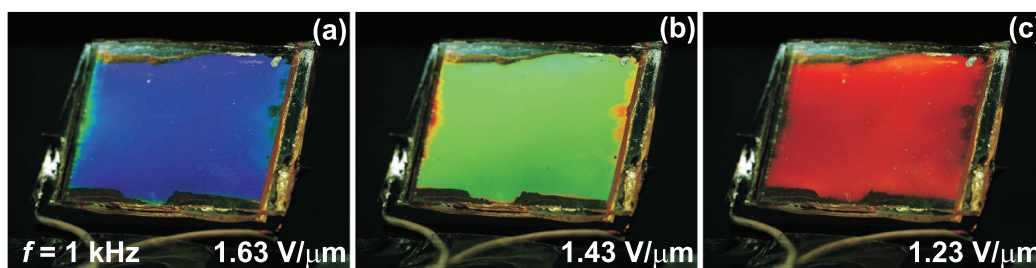


**Figure 11.** (Colour online) Photographs of the 22.1  $\mu\text{m}$  LC cell with  $\text{Ch}_{\text{OH}}$  formed under electric field: (a) 1.63  $\text{V}/\mu\text{m}$ , (b) 1.43  $\text{V}/\mu\text{m}$  and (c) 1.23  $\text{V}/\mu\text{m}$ . The temperature of the  $\text{Ch}_{\text{OH}}$  was 27.5  $^{\circ}\text{C}$ .

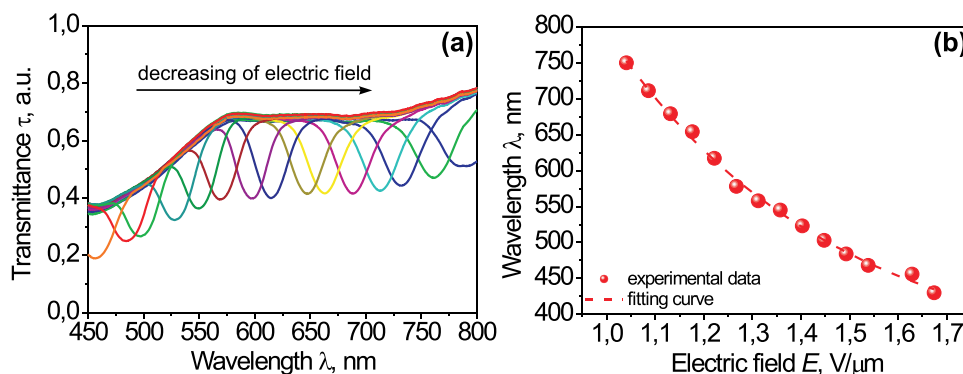


**Figure 12.** (Colour online) (a) Dynamics of the transmission spectrum of the  $\text{Ch}_{\text{OH}}$  under decreasing of the applied electric field  $E$ . (b) The dependence of the minimum of transmission spectrum of the  $\text{Ch}_{\text{OH}}$  in the visible light range on the applied electric field  $E$  of frequency  $f = 1$  kHz. LC cell was filled by  $\text{N}^*_{\text{tb}}$  mixture consisting of 10.1 wt. % ChD-3816. The temperature of the  $\text{Ch}_{\text{OH}}$  was 27.5  $^{\circ}\text{C}$ . The viewed angle of the LC cell was 45 $^{\circ}$ .

Figure 13 shows the dependence of the cholesteric pitch  $P_0$  of the  $\text{N}^*$  phase of the  $\text{N}^*_{\text{tb}}$ -forming mixture on the irradiation time  $t_{\text{irr}}$  (with no applied voltage). The gradual unwinding of cholesteric helix with irradiation time  $t_{\text{irr}}$  was observed, with a tendency to saturation (as it should be expected from the known data on similar systems [36,37]).

Under UV irradiation, the unwinding of the cholesteric helix leads to increasing of the value of the electric field  $E$  required to tune on the selective Bragg reflection in the visible range. Figure 14(a) shows the dependence of the critical electric field  $E_B$  on irradiation time  $t_{\text{irr}}$  for various concentrations  $C$  of the ChD-3816, namely 6.4 wt. % (red circles), 10.1 wt. % (green squares) and 12.2 wt. % (blue triangles) for  $\lambda_1 = 430$  nm (solid symbols) and  $\lambda_2 = 720$  nm (opened symbols).

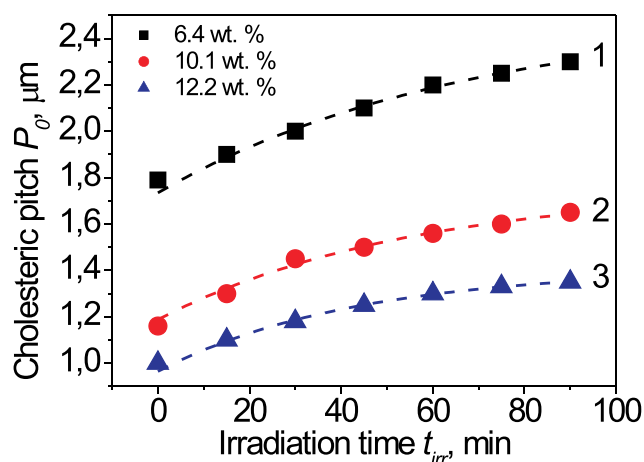
Figure 14(b) shows the electric field range  $\Delta E_B$  (i.e.  $\Delta E_B = E_B^{\lambda_1=430} - E_B^{\lambda_2=720}$ ) widened with prolonged UV exposure of the studied system. The prolonged UV illumination leads to broader  $\Delta E_B$ , which depends non-monotonously on the ChD-3816 concentration. The broadest  $\Delta E_B$  range is observed for  $C = 10.1$  wt. %, as can be seen from Figure 14(b).

Figure 15 shows the effect of the irradiation time  $t_{\text{irr}}$  on temperatures of phase transitions of the studied  $\text{N}^*_{\text{tb}}$ -

forming systems with different concentrations of the light-sensitive ChD-3816. The increasing of the irradiation time  $t_{\text{irr}}$  leads to monotonous decreasing of temperatures of phase transitions for both the  $\text{N}^*_{\text{tb}} - \text{N}^*$  (Figure 15(a)) and the  $\text{N}^* - \text{Iso}$  (Figure 15(b)), which is caused by *trans-cis* isomerisation of ChD-3816 molecules.

In the non-irradiated area the concentration of *trans*-isomer of the ChD-3816 is higher in comparison with the irradiated area. Due to this, the temperatures of phase transition  $\text{N}^*_{\text{tb}} - \text{N}^*$  are different in these areas. The appearance of selective Bragg reflection of the  $\text{Ch}_{\text{OH}}$  state in electric field  $E$  at the temperature near to phase transition  $\text{N}^*_{\text{tb}} - \text{N}^*$  will be observed at lower temperature in comparison with non-irradiated area. This can be used to obtain high contrast at the boundary between the irradiated and non-irradiated areas (Figure 16).

Photos of samples with the highest contrast of the images recorded by UV irradiation are shown in Figure 16. Owing to the reversible *trans-cis* isomerisation of ChD-3816 molecules, the  $\text{N}^*_{\text{tb}}$  phase, possessing  $\text{Ch}_{\text{OH}}$  state in wide temperature and electrically controllable ranges, can be used to re-recording of information (e.g. Figure 16(a-d)).



**Figure 13.** (Colour online) Helical pitch  $P_0$  as function of the irradiation time  $t_{irr}$  in the  $N^*$  phase of the  $N^*_{tb}$ -forming mixture at different concentrations of ChD-3816: (1) – 6.4 wt. % (solid black squares), (2) – 10.1 wt. % (solid red circles) and (3) – 12.2 wt. % (solid blue triangles). UV lamp with  $\lambda_{max} = 365$  nm and intensity (energy illuminance) in the plane of LC cell  $I \sim 14$  mW/cm<sup>2</sup> was used. The temperature of  $N^*$  phases was 34 °C.

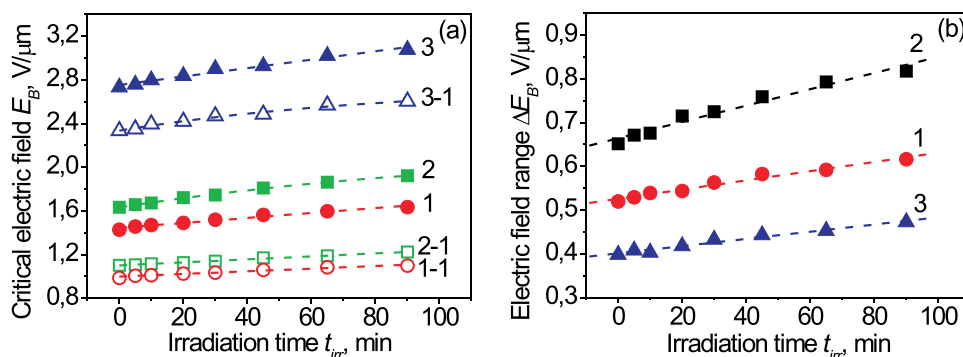


**Figure 14.** (Colour online) Dependence of the critical electric field  $E_B$  (a) and width of the electric field range  $\Delta E_B$  (b) on irradiation  $t_{irr}$  for the basic  $N_{tb}$ -forming mixture doped by ChD-3816 with various concentrations: (1) – 6.4 wt. % (red circles), (2) – 10.1 wt. % (green squares) and (3) – 12.2 wt. % (blue triangles). (a) The critical electric field  $E_B$  was measured at  $\lambda_1 = 430$  nm (closed symbols) and  $\lambda_2 = 720$  nm (opened symbols) at 34 °C. (b) The width of the electric field range  $\Delta E_B$  was calculated as difference between the critical electric field  $E_B$  measured at 430 nm and 720 nm for ChD-3816 concentrations: 6.4 wt. % (red circles, line 1), 10.1 wt. % (black squares, line 2) and 12.2 wt. % (blue triangles, line 3). The irradiation of LC cells was carried out by UV lamp with  $\lambda_{max} = 365$  nm and intensity (energy illuminance) in the plane of LC cell  $I \sim 14$  mW/cm<sup>2</sup>.

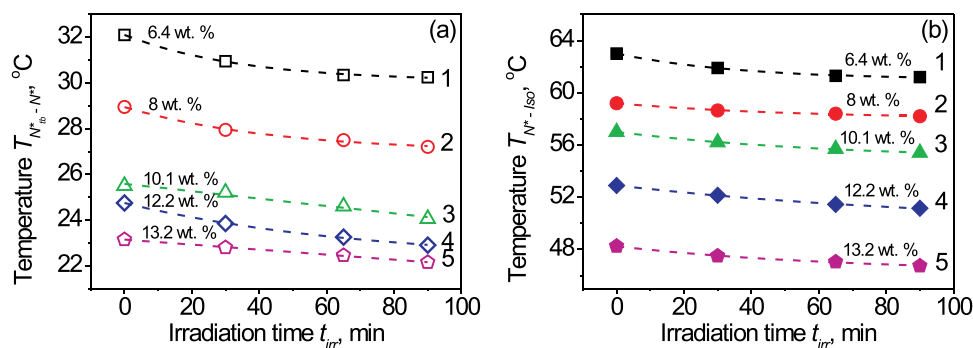


**Figure 15.** (Colour online) Dependence of the average temperatures of the phase transitions of  $N^*_{tb}$  (e.g. during heating and cooling process) on irradiation time  $t_{irr}$  for: (a)  $N^*_{tb}$  to  $N^*$  (opened symbols) and (b)  $N^*$  to Iso (solid symbols). The basic  $N^*_{tb}$  contains various concentrations of the light-sensitive ChD-3816, namely: (1) – 6.4 wt. % (black squares), (2) – 8 wt. % (red circles), (3) – 10.1 wt. % (green triangles), (4) – 12.2 wt. % (blue diamonds) and (5) – 13.2 wt. % (magenta pentagons). Irradiation of  $N^*_{tb}$  was carried out by UV lamp with  $\lambda_{max} = 365$  nm ( $I \sim 14$  mW/cm<sup>2</sup>) for various irradiation time  $t_{irr}$ : 30, 65 and 90 min. The rate of the temperature change during the heating/cooling process was 0.1 °C/min.

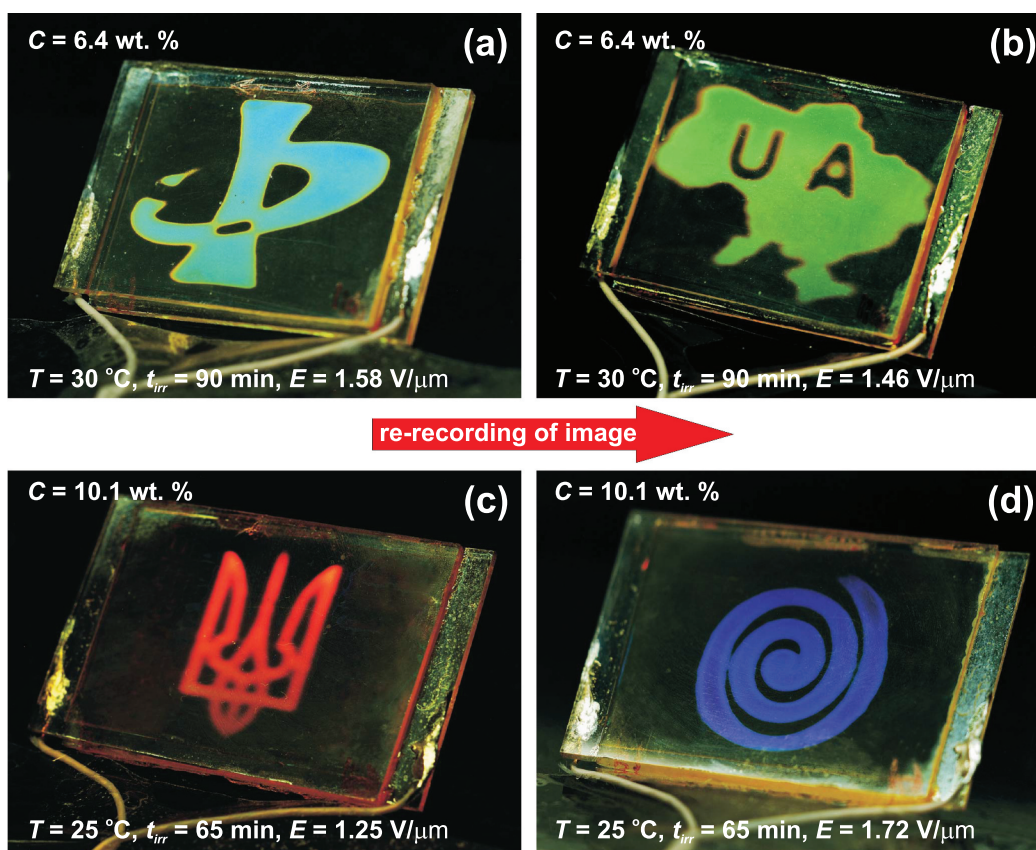


**Figure 16.** (Colour online) Photographs of samples with high contrast images recorded by UV irradiation for  $N^*_{tb}$ -forming systems with different concentration of ChD-3816.

#### 4. Conclusion

In this manuscript we studied light-sensitive chiral nematic twist-bend phase  $N^*_{tb}$ , consisting of basic nematic twist-bend  $N_{tb}$  mixture (*i.e.* two twist-bend nematic phases of achiral liquid crystals dimers, namely 1',7"-bis-4-(4-cyanobiphen-4'-yl)heptane (CB7CB), 1-(4-cyanobiphenyl-4'-yloxy)-6-(4-cyanobiphenyl-4'-yl)hexane (CB6OCB) and monomer nematic 4-pentyl-4'-cyanobiphenyl (K15 or 5CB) in weight ratio of (39:19:42) doped by a newly synthesised light-sensitive chiral dopant (1R,2S,5R)-2-isopropyl-5-methylcyclohexyl-4- $\{(E)$ -[4-(hexanoyloxy)phenyl]diazanyl}benzoate (ChD-3816). The concentration dependence and influence of UV irradiation on temperatures of phase transitions were studied. The decrease of the phase transition temperatures both with increasing concentration the ChD-3816 and irradiation time was found. At certain concentrations of the ChD-3816 there exists a wide temperature interval of  $N^*$  phase where oblique heliconical cholesteric state with selective Bragg reflection in the visible light spectrum can be observed. The critical electric field required to tune on the selective reflection in the visible range increases with increasing of the temperature of  $N^*$  phase and irradiation time. It has been also shown how the use of light-sensitive chiral dopants can

significantly expand the possibilities of wavelength tuning not only by means of the applied electric field but also using the light, thus opening prospects of new 'photo-electro-optical' effects in liquid crystals.

#### Acknowledgments

The authors are incredibly grateful to the Commander in-Chief of the Armed Forces of Ukraine General V. F. Zaluzhnyi, Ukrainian soldiers, volunteers, NATO countries and other allies of Ukraine, who support our country during full-scale war in Ukraine. This study was supported by the National Academy of Medical Sciences of Ukraine within project No. 0120U101532 and the National Academy of Sciences of Ukraine within project No. 0122U002636. The authors thank W. Becker (Merck, Darmstadt, Germany) for his generous gift of nematic liquid crystals E7. Dr. A. Buchnev (Cambridge, England) who had supplied us with polymer PI2555, and Field service specialist IV V. Danylyuk (Dish LLC, USA) for his gift of some Laboratory equipment. Mesogens CB7CB and CB6OCB were generously donated by the Materials and Manufacturing Directorate of the Air Force Research Laboratory, Wright-Patterson AFB, Ohio. The authors thank Prof. A. Tolmachev (Chemico-Biological Center Taras Shevchenko National University of Kyiv) and Dr. S. Lukyanets (Institute of Physics, NAS of Ukraine) for the helpful discussions.

## Disclosure statement

No potential conflict of interest was reported by the author(s).

## ORCID

Vitalii Chornous  <http://orcid.org/0000-0002-1431-6685>  
 Alina Grozav  <http://orcid.org/0000-0001-9821-0695>  
 Mykhailo Vovk  <http://orcid.org/0000-0003-1753-3535>  
 Daria Bratova  <http://orcid.org/0000-0002-3360-3188>  
 Natalia Kasian  <http://orcid.org/0000-0002-4739-2684>  
 Longin Lisetski  <http://orcid.org/0000-0003-4341-832X>  
 Igor Gvozдовskyy  <http://orcid.org/0000-0002-4531-9942>

## References

- [1] Planer J. Notiz über das Cholestein [note about the cholesterol]. *Annal Chem Pharm.* **1861**;118:25–27. German.
- [2] Shenderovskiy VA, Trokhymchuk AD, Lisetski LN, et al. Julius Planer. A pioneer in the study of liquid crystals. *J Mol Liq.* **2018**;267:560–563.
- [3] Reinitzer F. Beiträge zur Kenntniss des Cholesterins [contributions to the knowledge of cholesterol]. *Monatsh Chem.* **1888**;9:421–441. German.
- [4] Lehman O. Über fließende Kristalle [about flowing crystals]. *Z Phys Chem.* **1889**;4:462–472. German.
- [5] De Gennes PG, Prost J. *The physics of liquid crystals.* Oxford: Oxford Science Publications; **1993**.
- [6] Solladie' G, Zimmermann RG. Liquid crystals: a tool for studies on chirality. *Angew Chem Int Ed Engl.* **1984**;23:348–362.
- [7] Kitzerow HS, Bahr C. *Chirality in liquid crystals.* New York: Springer; **2001**.
- [8] Meyer RB. Effects of electric and magnetic fields on the structure of cholesteric liquid crystals. *Appl Phys Lett.* **1968**;12:281–282.
- [9] De Gennes PG. Calcul de la distorsion d'une structure cholesterique par un champ magnetique. *Solid State Commun.* **1968**;6:163–165.
- [10] Dozov I. On the spontaneous symmetry breaking in the mesophases of achiral banana-shaped molecules. *Europhys Lett.* **2001**;56:247–253.
- [11] Lisetski LN, Tolmachev AV. Invited lecture. Helical twisting in cholesteric mesophases: molecular structure and microscopic description. *Liq Cryst.* **1989**;5:877–888.
- [12] Cestari M, Diez-Berart S, Dunmur DA, et al. Phase behavior and properties of the liquid-crystal dimer 1',7"-bis(4-cyanobiphenyl-4'-yl)heptane: a twist-bend nematic liquid crystal. *Phys Rev E.* **2011**;84:031704.
- [13] Borshch V, Kim YK, Xiang J, et al. Nematic twist-bend phase with nanoscale modulation of molecular orientation. *Nat Commun.* **2013**;4:2635.
- [14] Chen D, Porada JH, Hooper JB, et al. Chiral heliconical ground state of nanoscale pitch in a nematic liquid crystal of achiral molecular dimers. *Proc Nat Acad Sci USA.* **2013**;110:15931–15936.
- [15] Xiang J, Shiyanovskii SV, Imrie C, et al. Electrooptic response of chiral nematic liquid crystals with oblique helicoidal director. *Phy Rev Lett.* **2014**;112:2017801.
- [16] Xiang J, Li Y, Li Q, et al. Electrically tunable selective reflection of light from ultraviolet to visible and infrared by helicoidal cholesterics. *Adv Mater.* **2015**;27:3014–3018.
- [17] Iadlovskaya OS, Maxwell GR, Babakhanova G, et al. Tuning selective reflection of light by surface anchoring in cholesteric cells with oblique helicoidal structures. *Opt Lett.* **2018**;43:1850–1853.
- [18] Mrukiewicz M, Iadlovskaya OS, Babakhanova G, et al. Wide temperature range of an electrically tunable selective reflection of light by oblique helicoidal cholesteric. *Liq Cryst.* **2019**;46:1544–1550.
- [19] Lavrentovich OD. Electromagnetically tunable cholesterics with oblique helicoidal structure. *Opt Mat Express.* **2020**;10:2415–2424.
- [20] Nava G, Ciciulla F, Simoni F, et al. Heliconical cholesteric liquid crystals as electrically tunable optical filters in notch and bandpass configurations. *Liq Cryst.* **2021**;48:1534–1543.
- [21] Liu B, Yuan C-L, Hu H-L, et al. Dynamically actuated soft heliconical architecture via frequency of electric fields. *Nat Commun.* **2022**;13:2712.
- [22] Thapa K, Iadlovskaya OS, Bisoyi HK, et al. Photocontrol of selective light reflection by oblique helicoidal cholesteric. In: Khoo IC, editor. *Proceedings of the Conference Liquid Crystals XXV; 2021 August 1-5; San Diego (CA): SPIE; 2021.* 11807. p. 118070X-1–8. DOI: [10.1117/12.2592765](https://doi.org/10.1117/12.2592765).
- [23] Thapa K, Iadlovskaya OS, Bisoyi HK, et al. Combined electric and photocontrol of selective light reflection at an oblique helicoidal cholesteric liquid crystal doped with azoxybenzene derivative. *Phys Rev E.* **2021**;104:04702.
- [24] Yuan G-L, Huang W, Zheng Z-G, et al. Stimulated transformation of soft helix among helicoidal, heliconical, and their inverse helices. *Sci Adv.* **2019**;5:eaax9501.
- [25] Matsuyama A. Field-induced oblique helicoidal cholesteric phases in mixtures of chiral and achiral liquid crystalline molecules. *Liq Cryst.* **2017**;45:153–164.
- [26] Kasian NA, Lisetski LN, Gvozдовskyy IA. Twist-bend nematics and heliconical cholesterics: a physico-chemical analysis of phase transitions and related specific properties. *Liq Cryst.* **2022**;49:142–152.
- [27] Jokisaari JP, Luckhurst GR, Timimi BA, et al. Twist-bend nematic phase of the liquid crystal dimer CB7CB: orientational order and conical angle determined by <sup>129</sup>Xe and <sup>2</sup>H NMR spectroscopy. *Liq Cryst.* **2015**;42:708–721.
- [28] Čopič M, Mertelj A. Q-tensor model of twist-bend and splay nematic phases. *Phys Rev E.* **2020**;101:022704.
- [29] Peterson DA, Gao M, Kim Y-K, et al. Understanding the twist-bend nematic phase: the characterisation of 1-(4-cyanobiphenyl-4'-yloxy)-6-(4-cyanobiphenyl-4'-yl)hexane (CB6OCB) and comparison with CB7CB. *Soft Mater.* **2016**;12:6827–6840.

- [30] Walker R, Pocięcha D, Storey JMD, et al. The chiral twist-bend nematic phase ( $N_{TB}$ ). *Chem Eur J.* **2019**;25:13329–13335.
- [31] Paterson DA, Abberley JP, Harrison WTA, et al. Cyanobiphenyl-based liquid crystal dimers and the twist-bend nematic phase. *Liq Cryst.* **2017**;44:127–146.
- [32] Babakhanova G, Parsouzi Z, Paladugu S, et al. Elastic and viscous properties of the nematic dimer CB7CB. *Phys Rev E.* **2017**;96:062704.
- [33] HD MicroSystems product bulletin PI2525, PI2555 and PI2574; **2012** November.
- [34] Senyuk BI, Smalyukh II, Lavrentovich OD. Undulations of lamellar liquid crystals in cells with finite surface anchoring near and well above the threshold. *Phys Rev E.* **2006**;74:011712.
- [35] Tuchband MR. Revealing the nanoscale structure and behavior of the twist-bend nematic liquid crystal phase [dissertation]. Boulder (CO): University of Colorado Boulder; **2018**.
- [36] Arozon D, Levy EP, Collings PJ, et al. *Trans-cis* isomerisation of an azoxybenzene liquid crystal. *Liq Cryst.* **2007**;34:707–718.
- [37] Serbina MI, Kasian NA, Lisetski LN. Helical twisting in nemato-cholesteric systems based on cholesterol derivatives and photosensitive azoxy compounds. *Crystallogr Rep.* **2013**;58:155–159.